Chiral Cyclobutane-Based Ureas as Versatile Platforms to Tune Structural Diversity: An Experimental and Theoretical Approach

Ona Illa,[a,*] Eric Da Silva,[a] Elisabeth Torres,[a] Ángel Álvarez-Larena,[b] Klaus Wurst,[c] Rosa M. Ortuño,[a] Vicenç Branchadell[a,*]

a O. Illa, E. Da Silva,[&] E. Torres,[£] R. M. Ortuño, V. Branchadell.
Departament de Química, Universitat Autònoma de Barcelona, 08193 Cerdanyola del Vallès, Spain
ona.illa@uab.cat ; vicenc.branchadell@uab.cat
[&] *Present address*: SNF, Lyon
[£] *Present address*: Berry Global, Inc., c/ Tuset, 23, 08006 Barcelona, Spain.

b Á. Álvarez-Larena
Servei de Difracció de RX, Universitat Autònoma de Barcelona, 08193 Cerdanyola del Vallès, Spain.

c K. Wurst
Institut für Allgemeine Anorganische und Theoretische Chemie, Universität Innsbruck, A-6020, Innrain 80-82, Austria.

ABSTRACT

Four new chiral 2,2'-disubstituted biscyclobutane ureas have been synthesized and crystallized. Each of them bears a different substituent on positions 2,2', *i.e.* esters, hydroxymethyl groups and carboxyl groups. The mode of aggregation of each urea in the crystal packing to form chains, helices, sheets, and others, is tuned both by the intermolecular hydrogen bonds between the urea groups and by the different ability of the substituents to generate extra hydrogen bonding. Experimental results have been rationalized with the aid of computational calculations, which allow to understand the contribution of the energetic factors to the stabilization of the preferential structures observed.

1. INTRODUCTION

Chiral organic ureas are compounds of relevance in several fields. Their behavior as bidentate ligands bearing an electron-donor center (the carbonyl oxygen) and two acidic protons confers them with singular properties to be used for several purposes. For instance, they are employed as organocatalysts to activate and induce asymmetry in several reactions due to their ability to coordinate simultaneously with an electrophile and a nucleophilic reagent, as well as for hydrogen bonding.[1,2,3,4,5,6] Another substantial use of ureas is in the field of molecular recognition, especially in host-guest interactions.[7,8,9,10]

From a structural point of view, investigations on the behavior of ureas as inductors of chirality have shown the ability of urea-based oligomers to fold and to self-assemble mimicking natural biopolymers. For example, Hamilton et al. have described benzoylurea oligomers as synthetic foldamers that mimic extended α– helices.[11,12] Guichard et al. have reported on the ability of oligomeric chiral ureas to fold.[13,14] They also described folding-induced axial organization of urea helices in such a way that H-bonded assembly of helices resulted in supramolecular helices.[15,16,17] Ureas have also been described as good gelators.[9] For instance, bisurea gelators derived from 1,6-diaminopyridine have been developed and described to efficiently gelate common organic and liquid crystalline solvents. The resulting hydrogen bonded structures exhibit good electrooptic properties making the urea gelators useful as components of functional soft materials.[18] On the other hand, C_3-symmetrical supramolecular architectures, such as fibers and organic gels, result from discotic trisureas. In this case, π,π-stacking interactions between aromatic rings play a crucial role in the molecular axial pilling.[19]

In general, weak interactions such as hydrogen bonding, π,π-interactions, C-H···π interactions, salt bridges, amongst others, have been proven to be of critical importance in the self-assembly and recognition of solid-state structures.[20]

N,N-disubstituted ureas mostly adopt a *trans,trans* arrangement and often form supramolecular chains by the formation of two N*H*···*O*C hydrogen bonds between every two neighboring molecules.[21]

There are basically two models for these supramolecular chains. One of them is characterized by having the carbonyl groups aligned (Figure 1a). In fact, in symmetrical ureas, with the same substituent on each nitrogen atom, it is relatively common to find internal symmetry in the chain, with a twofold axis containing the CO groups (see for instance, CYHXUR,[22] Figure 2a). In most cases, the urea groups (NCON) of the chain units are coplanar, but not always (see YUZHUY,[23] Figure 2b). The second set of supramolecular chains includes structures whose chains have the carbonyl groups away from colinearity and the planes described by the urea groups forming angles different from 0 degrees (see IQUZOM,[24] Figure 2c).

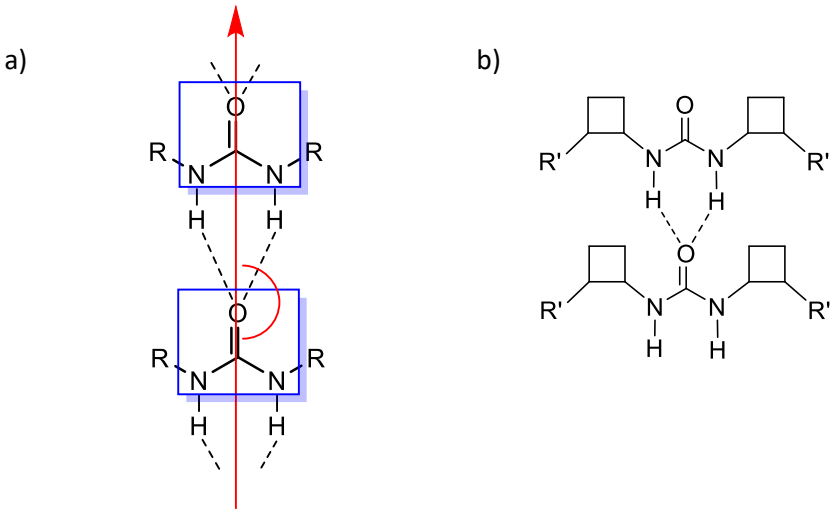

Figure 1. a) *trans,trans*-Arrangement of substituents in a *N,N*-disubstituted urea and straight chains formed as the result of two intermolecular N*H*···*O*C hydrogen bonds. The hypothetical axis containing all CO bonds is represented in red and the planes containing each urea group in blue; b) General structure of the ureas studied in this work and schematic representation of an aggregate of two urea molecules.

Some chiral *N*,*N*′-disubstituted ureas have a specific feature: they form helical chains which are symmetrical about enantiomorphic screw axes. Chains with the carbonyl groups not aligned with the screw axis are more common (see HAWLIB,[25] Figure 2d) but it is possible to find also chains with the carbonyl group aligned with the screw axis (CUNCEU,[26] Figure 2e).

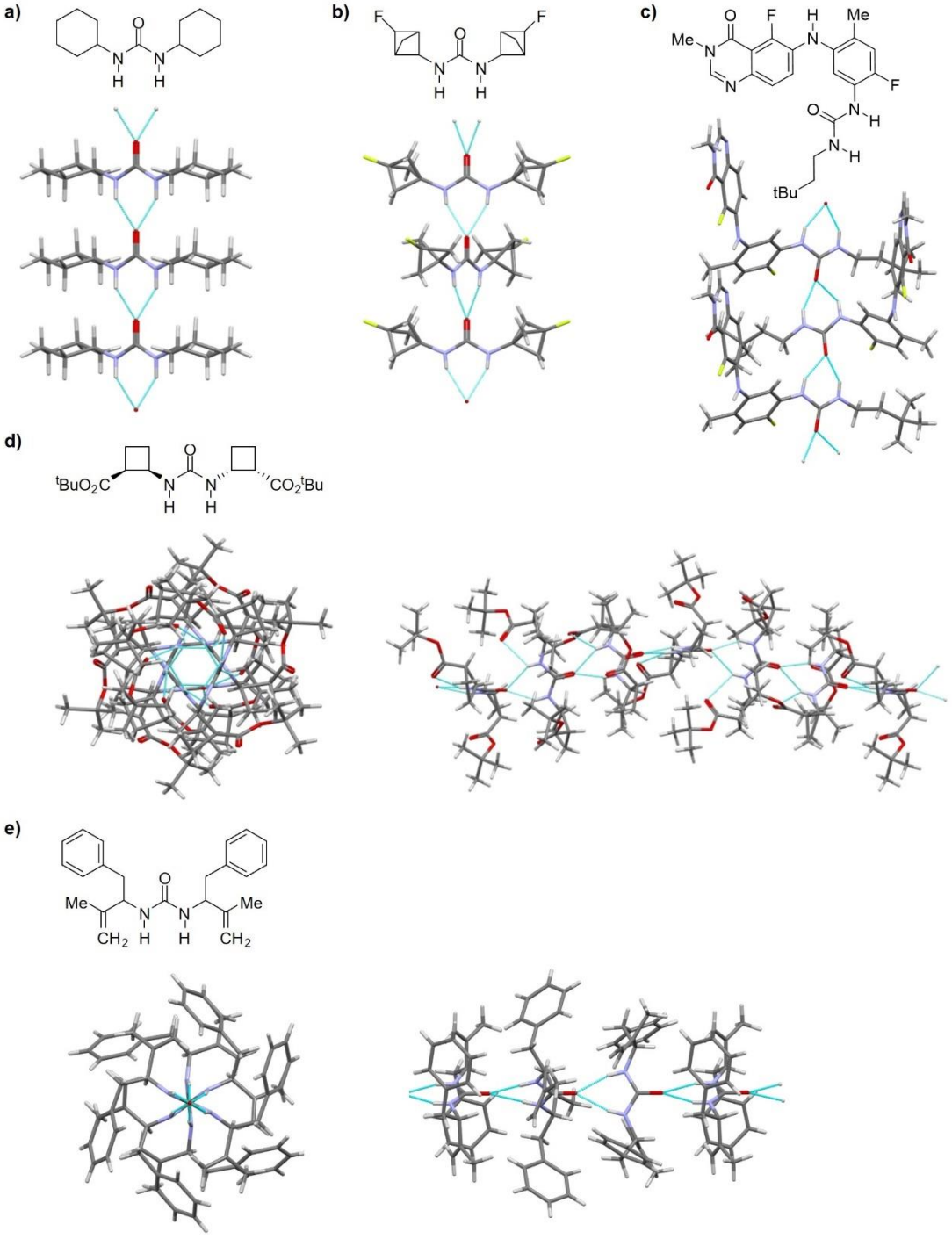

Figure 2. Examples of urea crystalline structures forming 1D infinite chains by the formation of two N*H*···*O*C hydrogen bonds: a) CYHXUR,[22] carbonyl groups aligned and included in a twofold axis, coplanar urea groups; b) YUZHUY,[23] carbonyl groups aligned and included in a twofold axis, non-coplanar urea groups; c) IQUZOM,[24] non-aligned carbonyl groups and non-coplanar

urea groups; d) HAWLIB,[25] helical chain with non-aligned carbonyl groups; e) CUNCEU,[26] helical chain with aligned carbonyl groups and non-coplanar urea groups.

The chiral 1,2-disubstituted cyclobutane moiety has been successfully incorporated in designed peptide foldamers based on cyclobutane β-amino acids to induce well defined secondary structures in solution[27] and in the solid-state.[28] The conformational restrictions imposed by the severe constrain of the cyclobutane ring are responsible for the conformational bias of these compounds. Some cyclobutane-based peptidomimetics,[29] and other derivatives, bearing ester or amide functions, with properties as surfactants[30,31] or organogelators[32] have shown their ability to self-assemble into ordered aggregates and/or to gelate some common organic solvents.

We have investigated the structural properties of cyclobutane-containing ureas as powerful tools to tune the supramolecular structural diversity. Herein, we describe the versatile and stereoselective synthesis of chiral biscyclobutane ureas bearing functional groups at the 2,2'-positions, which influence their molecular conformations and the supramolecular arrangements in the solid state. Figure 1b shows the general structure of the compounds considered. In particular, we have taken into account the colinearity of the CO groups, and the angle (τ) between the mean planes described by the urea groups (NCON) of one molecule and the following one, which gives an idea about the distortion of the coplanarity of the successive urea molecules and about the helicity of the aggregates. Results of X-ray diffraction analysis of these molecules account for electronic and steric factors playing a crucial role in the formation of crystal structures. Besides these features, computational calculations provide a rationale for the observed crystallographic results.

2. EXPERIMENTAL SECTION

2.1. Chemicals and materials. The chemicals and reagents (Sigma-Aldrich, Fluka) were of analytical grade and were used without further purification. Anhydrous dichloromethane was freshly distilled when needed under a nitrogen atmosphere from calcium chloride. Anhydrous acetone was freshly distilled from calcium chloride and anhydrous toluene was freshly distilled from sodium/benzophenone. TLC on silica gel-coated aluminum plates was performed in the systems indicated for each product in the following description. The compounds were visualized by exposure to UV light at 254 nm, dipping in a basic potassium permanganate solution or in an acid vanillin solution. Flash chromatography purifications were carried out on silica gel (200-400 mesh). Melting points were recorded on a Reicher Kofler block and values are uncorrected. ^{1}H-NMR and ^{13}C-NMR spectra were measured on a Bruker DPX250 spectrometer. Chemical shifts are reported in parts per million. IR spectra were obtained from samples in neat form with an ATR (Attenuated Total Reflectance) accessory. High resolution mass spectra were recorded using an ESI-MS QTOF apparatus.

2.2. Synthesis. ***2.2.1. (1R,1'R,2S,2'S)-Dimethyl-2,2'-(carbonyldiimino)-dicyclobutanecarboxylate,*** **2**: Ethyl chloroformate (0.53 mL, 5.57 mmol) and freshly distilled triethylamine (0.72 mL, 5.16 mmol) were successively added to a solution of half ester **1**[33] (680 mg, 4.3 mmol) in anhydrous acetone (20 mL). The mixture was stirred at room temperature for 30 minutes. A solution of sodium azide (647 mg, 9.95 mmol) in water (15 mL) was added and the mixture was stirred for 1.5 hours. The solvent was removed under vacuum and the residue was poured into CH_2Cl_2 (20 mL). The organic phase was washed with saturated aqueous $NaHCO_3$ (2 x 20 mL). The organic layer was dried over $MgSO_4$, filtered, and evaporated. *Warning*: This product should be carefully manipulated because of its explosive nature. Anhydrous toluene (20 mL) was added to

the residue and the mixture was heated to reflux for 2 hours. After cooling, the solvent was removed under vacuum to afford an orange solid. The solid was dissolved in a 1:1 mixture of THF/water (50 mL) and was stirred overnight at room temperature. After evaporating the solvent, the residue was purified by column chromatography on neutral silica gel (1:1 mixture of ethyl acetate-hexane) to afford pure **2** (290 mg, 1.02 mmol, 47% yield). Crystals, m.p. 164-166 ºC (from ethyl acetate-pentane); $[\alpha]_D^{20}$ = -173 (*c* = 0.53 in CH_2Cl_2); ^{1}H-NMR (250 MHz, $CDCl_3$, 25°C): δ=5.39 (broad s, 2H), 4.62 (m, 2H), 3.71 (s, 6H), 3.40 (m, 2H), 2.24-2.35 (m, 4H), 1.90-2.02 (m, 4H); ^{13}C-NMR (62.5 MHz, $CDCl_3$, 25°C): δ=175.2, 155.7, 51.6, 45.3, 30.0, 18.6; IR (ATR): ν=3300, 2950, 1725, 1715, 1650 cm^{-1}; Elemental analysis calcd (%) for $C_{13}H_{20}N_2O_5$: C 54.92, H 7.09, N 9.85, O 28.14 found: C 54.65, H 7.22, N 9.95, O 28.18.

2.2.2. (1R,1'R,2S,2'S)-2,2'-(Carbonyldiimino)dicyclobutanecarboxylic acid, **3**: Urea **2** (100 mg, 0.35 mmol) was stirred in a solution of 0.25 M NaOH in water (5 mL) and THF (1 mL) at 0 ºC for 2 hours. 1 M HCl was added to the solution until it reached pH 3. The solution was evaporated to dryness under vacuum giving a white powder. Ethanol (2 x 10 mL) was added and heated at reflux. The mixture was filtered in hot ethanol. The filtrate was evaporated under vacuum to afford **3** (65 mg, 0.25 mmol, 72% yield). Crystals, m.p. 183-185 ºC (from ethanol); $[\alpha]_D^{20}$ = -100 (*c* = 0.2 in MeOH); ^{1}H-NMR (250 MHz, MeOH-d_4, 25°C): δ=4.93 (broad s, 2H), 4.53 (q, ^3J(H,H) = 9.5 Hz, 2H), 3.32 (m, 2H), 2.19-2.31 (m, 4H), 1.85-2.00 (m, 4H); ^{13}C-NMR (62.5 MHz, MeOH-d_4, 25°C): δ=175.9, 157.7, 46.2, 45.8, 29.0, 17.9; IR (ATR): ν=3373, 2955, 1730, 1676, 1544, 1235 cm^{-1}; HRMS (ESI) *m/z:* $[M-H]^-$ Calcd for $C_{11}H_{14}N_2O_5$: 255.0986; Found: 255.0984.

2.2.3. (1R,1'R,2S,2'S)-Hydroxymethyl-2,2'-(carbonyldiimino)dicyclobutane, **4**: Urea **2** (160 mg, 0.56 mmol) was dissolved in a 2:1 mixture of THF/water (8.3 mL) at 0 ºC. Then

$NaBH_4$ (105 mg, 2.78 mmol) was added. The mixture was allowed to reach room temperature and stirred overnight. The solvent was evaporated under vacuum until dryness and the residue was directly purified by column chromatography on neutral silica gel (9:1 CH_2Cl_2-MeOH) to afford pure **4** (80 mg, 0.35 mmol, 63% yield). Crystals, m.p. 179-181 ºC (from CH_2Cl_2/MeOH); $[\alpha]_D^{20}$ = -98 (*c* = 0.42 in MeOH); ^{1}H-NMR (250 MHz, MeOH-d_4, 25°C): δ=4.28 (q, , ^3J(H,H) = 7.0 Hz, 2H), 3.60-3.78 (m, 4H), 2.66 (m, 2H), 2.33 (m, 2H), 1.85-2.00 (m, 4H), 1.62-1.68 (m, 2H); ^{13}C-NMR (62.5 MHz, MeOH-d_4, 25°C): δ=160.4, 62.7, 47.6, 43.1, 28.9, 19.3; IR (ATR): ν=3330, 2940, 2869, 1625, 1556, 1250, 1030 cm^{-1}; HRMS (ESI) *m/z:* $[M+Na]^+$ Calcd for $C_{11}H_{20}N_2NaO_5$: 251.1366; Found: 251.1376.

2.2.4. (1R,1'R,2S,2'S)-Dibenzyl-2,2'-(carbonyldiimino)dicyclobutanecarboxylate, **5**: Urea **3** (115 mg, 0.45 mmol) was dissolved in anhydrous DMF (3 mL). Cs_2CO_3 (294 mg, 0.90 mmol) and benzyl bromide (0.16 mL, 1.35 mmol) were subsequently added. The mixture was stirred at room temperature overnight. Ethyl acetate (10 mL) was then added, and the organic layer was washed with a saturated aqueous solution of $NaHCO_3$ (5 x 5 mL). The organic layer was dried over anhydrous magnesium sulfate and the solvent evaporated under vacuum. The excess of benzyl bromide was lyophilized using a dry-freezer. The crude material was the purified by column chromatography in neutral silica gel (2:1 ethyl acetate-hexane) to afford **5** (90 mg, 0.21 mmol, 46% yield). Crystals, m.p. 119-122 ºC (from ethyl acetate-pentane); $[\alpha]_D^{20}$ = -172 (*c* = 0.27 in CH_2Cl_2); ^{1}H-NMR (250 MHz, $CDCl_3$, 25°C): δ=7.36 (m, 10H), 5.13 (m, 6H), 4.61 (m, 2H), 3.37 (m, 2H), 2.15-2.32 (m, 4H), 1.92-1.97 (m, 4H); ^{13}C-NMR (62.5 MHz, $CDCl_3$, 25°C): δ=174.4, 155.3, 135.9, 128.6, 128.3, 128.2, 66.3, 45.5, 45.3, 30.1, 18.5; IR (ATR): ν=3331, 2924, 1725, 1638, 1556, 1165 cm^{-1}; HRMS (ESI) *m/z:* $[M+Na]^+$ Calcd for $C_{25}H_{28}N_2NaO_5$: 459.1890; Found: 459.1891.

***2.2.5. (1S,2R)-1-Benzyl-2-methylcyclobutane-1,2-dicarboxylate,* 6:** Hemiester **1**[33] (490 mg, 3.1 mmol) and cesium carbonate (1.23 g, 3.8 mmol) were stirred in anhydrous DMF (10 mL) under nitrogen atmosphere at room temperature during 1 hour. Benzyl bromide (0.45 mL, 3.9 mmol) was added, and the mixture was stirred overnight at room temperature. The mixture was extracted with ethyl acetate (30 mL) and washed several times with $NaHCO_3$ (3 x 30 mL). The organic layer was dried with magnesium sulfate and evaporated under vacuum. The crude was purified by column chromatography on neutral silica gel (2:1 ethyl acetate-hexane) to afford pure **6** as an oil (561 mg, 2.3 mmol, 73% yield). $[\alpha]_D^{20}$ = -36 (*c* = 0.87 in CH_2Cl_2). ^{1}H-NMR (250 MHz, $CDCl_3$, 25°C): δ=7.37 (m, 5H), 5.13 (s, 2H), 3.54 (s, 3H), 3.42 (m, 2H), 2.4 (m, 2H), 2.2 (m, 2H). ^{13}C-NMR (62.5 MHz, $CDCl_3$, 25°C): δ=173.5, 173.0, 135.9, 128.5, 128.4, 128.2, 66.4, 51.4, 40.6, 40.5, 22.1. IR (ATR): ν=2892, 1737, 1436, 1243 cm^{-1}. HRMS (ESI) *m/z:* $[M+Na]^+$ Calcd for $C_{14}H_{16}NaO_4$: 271.0941; Found: 271.0945.

***2.2.6. (1S,2R)-2-(Benzyloxycarbonyl)cyclobutanecarboxylic acid,* 8**: Diester **6** (447 mg, 1.8 mmol) was added to a solution of 0.25 M NaOH (10 mL) and THF (2 mL). The mixture was stirred at 0 ºC for 1 hour. The crude was acidified to pH= 3-4 with 1 M HCl, and the product was extracted with ethyl acetate (3 x 10 mL). The organic layer was dried with magnesium sulfate and the solvent was removed under vacuum. The residue was purified by column chromatography on neutral silica gel (2:8 ethyl acetate-hexane) to afford **8**[34] as an oil (177 mg, 0.8 mmol, 42% yield). $[\alpha]_D^{20}$ = -17 (*c* = 0.55 in CH_2Cl_2). ^{1}H-NMR (250 MHz, $CDCl_3$, 25°C): δ=7.30 (m, 5H), 5.10 (d, 2H), 3.48 (m, 2H), 2.43 (m, 2H), 2.24 (m, 2H). ^{13}C-NMR (62.5 MHz, $CDCl_3$, 25°C): δ=179.0, 173.3, 136.2, 128.9, 128.7, 128.6, 67.0, 41.0, 40.9, 22.6, 22.5. IR(ATR): ν=2892, 1737, 1436, 1243 cm^{-1}. HRMS (ESI) *m/z:* $[M+Na]^+$ Calcd for $C_{13}H_{14}NaO_4$: 257.0784; Found: 257.0784.

2.2.7. (1S,1'S,2R,2'R)-dibenzyl-2,2'-(carbonyldiimino)dicyclobutanecarboxylate, *ent*-**5**: A mixture of ethyl chloroformate (0.1 mL,1.08 mmol) and freshly distilled Et_3N (0.15 mL, 1.08 mmol) were successively added to a solution of **8** (180 mg, 0.77 mmol) in anhydrous acetone (20 mL). The mixture was stirred at room temperature for 1 hour. A solution of NaN_3 (127 mg, 1.96 mmol) in water (15 mL) was added and the mixture was stirred for 1.5 hours. The solvent was removed under vacuum and the residue was poured into CH_2Cl_2 (20 mL). The organic layer was washed with saturated aqueous $NaHCO_3$ (2 x 20 mL). The organic layer was dried over $MgSO_4$, filtered off and evaporated. *Warning*: This product should be carefully manipulated because of its explosive nature. The residue was poured into 20 mL of anhydrous toluene (20 mL) and the mixture was heated to reflux for 2 hours. After cooling, the solvent was removed under vacuum, an orange solid being obtained. The solid was stirred in presence of a 1:1 mixture of THF/water (10 mL) overnight at room temperature. After evaporating the solvent, the residue was purified by column chromatography on neutral silica gel (1:1 THF-hexane) to afford *ent*-**5** as a white solid (81 mg, 0.18 mmol, 48% yield). m.p. 121-124 ºC (from ethyl acetate-pentane). $[\alpha]_D^{20}$ = +177 (*c* = 0.5 in CH_2Cl_2). ^{1}H-NMR (250 MHz, $CDCl_3$, 25°C): δ=7.36 (m, 10H), 5.13 (m, 6H), 4.61 (m, 2H), 3.37 (m, 2H), 2.15-2.32 (m, 4H), 1.92-1.97 (m, 2H); ^{13}C-NMR (62.5 MHz, $CDCl_3$, 25°C): δ=174.4, 155.3, 135.9, 128.6, 128.3, 128.2, 66.3, 45.5, 45.3, 30.1, 18.5. IR(ATR): ν=3322, 2980, 1720, 1625, 1550, 1155 cm^{-1}. HRMS (ESI) *m*/*z:* $[M+Na]^+$ Calcd for $C_{25}H_{28}N_2NaO_5$: 459.1890; Found: 459.1892.

2.3. Crystallographic Details. ***Single Crystal X-ray Diffraction.*** Single crystals of ureas **2**, **4**, and *ent*-**5** were obtained by crystallization from ethyl acetate-pentane, CH_2Cl_2/MeOH and ethyl acetate-pentane, respectively. Data were collected using Mo Ka radiation in a SMART-APEX diffractometer. Single crystal of **3** was measured on a Bruker D8 Quest diffractometer equipped with a Photon III C14 area detector. An

empirical absorption correction was applied (SADABS). The structures were solved by direct methods (SHELXS-86) and refined by full-matrix least-squares methods on F^2 for all reflections (SHELXL-2016). Non-hydrogen atoms were refined with anisotropic displacement parameters. Hydrogen atoms bonded to carbon atoms were placed in calculated positions with isotropic displacement parameters fixed at 1.5 (methyl hydrogen atoms) or 1.2 (the rest) times the U_{eq} of the corresponding carbon atoms. Hydrogen atoms bonded to oxygen or nitrogen atoms were localized in a difference Fourier map. For comparison of hydrogen bonds, in the last refinement cycles, the hydrogen atoms bonded to nitrogen atoms were placed in calculated positions with isotropic displacement parameters fixed at 1.2 times the U_{eq} of the corresponding nitrogen atoms, and the hydrogen atoms bonded to oxygen atoms were placed in calculated positions with isotropic displacement parameters fixed at 1.5 times the U_{eq} of the corresponding oxygen atoms and a rotating group refinement was used. Restraints were applied to some distances and displacement parameters of the benzenes of the urea *ent*-**5** to have reasonable values.

Crystal data and further refinement details are presented in Tables S1- S8 and in Figures S1-S4 in the Supporting Information (SI).

2.4. Computational Details. The structures of the ureas and their aggregates were optimized using M06-2X density functional[35] and the 6-31G(d) basis set. These calculations have been carried out using the Gaussian-09 program.[36] The energies of all optimized structures have been recalculated with the Def2TZVP basis set.[37] For the simplest model, the 6-311++G(d,p) basis set has also been used in the geometry optimization. The interaction between urea molecules has been analyzed using the Natural Bond Order (NBO) method.[38]

3. RESULTS AND DISCUSSION

3.1. Stereoselective synthesis of chiral 2,2'-disubstituted biscyclobutane ureas.

Scheme 1 shows the enantiodivergent synthetic route to different biscyclobutane ureas starting from half-ester **1**[33] as the common chiral precursor.

Product **1** was reacted with ethyl chloroformate to afford a mixed anhydride that was reacted with sodium azide. The resultant acyl azide was submitted to Curtius rearrangement by heating to reflux in anhydrous toluene and the produced isocyanate was reacted in situ with a 10:1 pyridine-water mixture to afford urea **2** in 47% overall yield from **1**. In turn, **2** was reduced with $NaBH_4$ in a 2:1 THF-water mixture to provide dihydroxymethyl derivative **4** in 63% yield. Alternatively, diester **2** was treated with 0.25 M NaOH, followed by acidification to pH 3-4, affording diacid **3** in 72% yield. Dibenzyl ester **5** was prepared by reaction of **3** with benzyl bromide and cesium carbonate (46% yield).

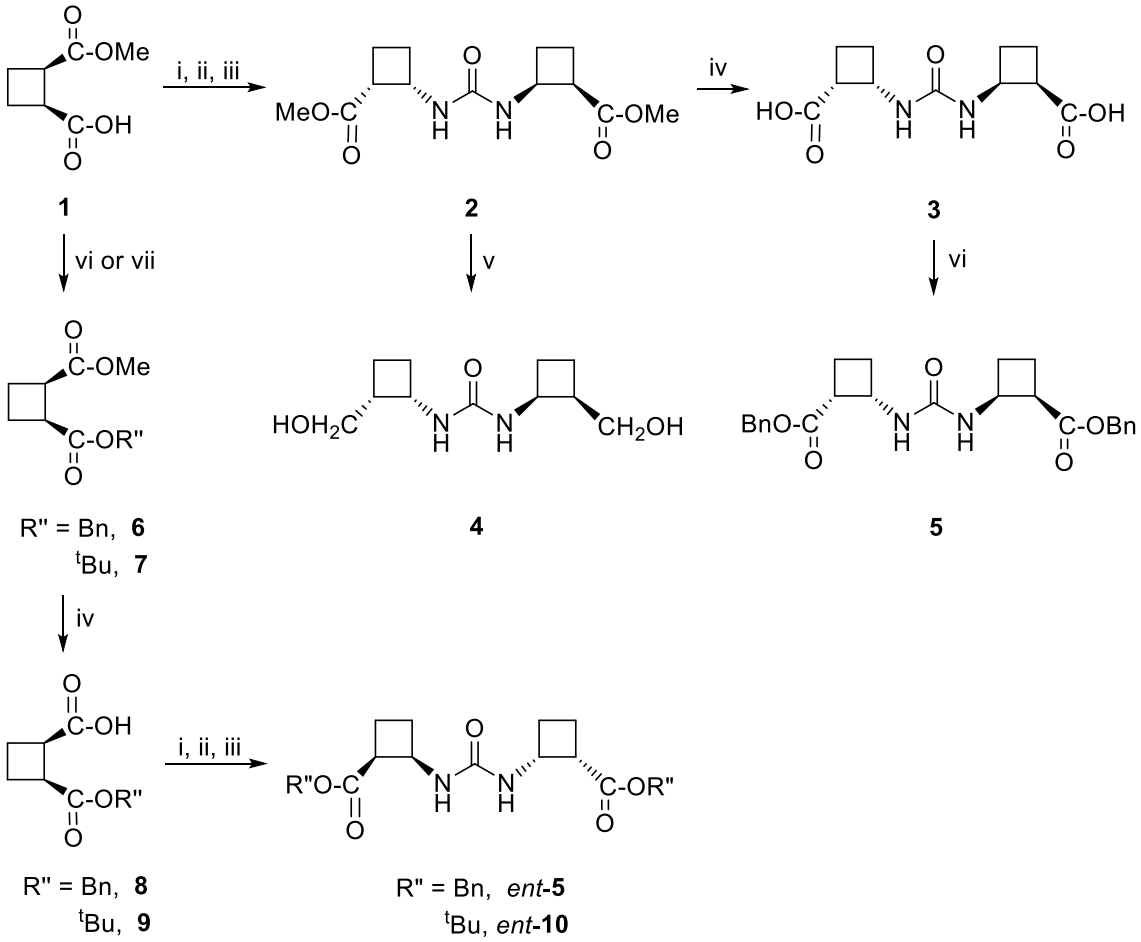

Scheme 1. Stereoselective synthesis of chiral biscyclobutane ureas. Reagents, conditions, and isolated yields: i) $ClCO_2Et$, Et_3N, acetone, rt, 30 min. ii) NaN_3, H_2O, rt, 1.5 h. iii) (a) toluene, reflux, 2 h. (b) 1:1 TFH-water, rt, overnight. Yield (three steps): 47% for **2**, 48% for *ent*-**5**, 35% for *ent*-**10**. iv) 0.25 M NaOH, THF-H_2O, 0 ºC, 2 h. 72% for **3**, 42% for **8**, quantitative for **9**. v) $NaBH_4$, 2:1 THF-H_2O, rt, overnight, 63%. vi) BnBr, Cs_2CO_3, DMF, rt, overnight. 46% for **5**, 73% for **6**. vii) Cl_3C-C(NH)O^{t}Bu, CH_2Cl_2, rt, overnight, 90%.

Ureas *ent*-**5** and *ent*-**10**, with an opposite chirality to ureas **2**-**5**, were synthesized as follows. Reaction of half-ester **1** with benzyl bromide and Cs_2CO_3 provided diester **6** (73% yield) that was submitted to selective saponification of the methyl ester affording half ester **8** (42% yield). Alternatively, treatment of **1** with *tert*-butyl trichloroacetimidate led to diester **7** that was converted into **9** following the protocols previously reported.[25] Finally, half esters **8** and **9** were transformed into ureas *ent*-**5** and *ent*-**10**, respectively, following a similar procedure to that used to prepare urea **2**. Compounds **7**, **9** and *ent*-**10**

were earlier described.[25] Urea *ent*-**10** had been formerly obtained as a by-product of a Curtius rearrangement, its identity being verified by X-ray diffraction analysis.

3.2. Structural study of the synthesized ureas. The structural study of these compounds was undertaken by means of X-ray crystallography and computational calculations that allowed us to understand their molecular conformations and crystal packings.

3.2.1. X-ray diffraction analysis. An accurate investigation was carried out to determine the structural arrangement of ureas **2**-**4** and *ent*-**5** in the solid state and to discern the influence of the functional groups located at the cyclobutane side chains (Figure 3 in the main text and Tables S1-S8 in the SI).

In the case of ureas **2** and *ent*-**5**, supramolecular chains with unaligned carbonyls (angles of 151º and 159º, respectively, as shown in Figures 3a and 3b) and non-coplanar urea groups are observed. The value of the angle between mean planes containing the urea groups of two consecutive molecules (τ) is 82º for **2** and 71º for *ent*-**5**. The overall distortion is greater in **2**, probably due to the presence of intermolecular bifurcated hydrogen bonds between the N*H* in one molecule and one of the oxygens of the ester group (CO*O*Me) in the following one (Figure 3a and Table S2 in the SI). In the case of urea *ent*-**5**, the presence of the bulky benzyl groups induces an aggregate disposition in which the distance between the N*H* of one molecule with one of the oxygens of the ester group of the following one (CO*O*Bn) is clearly larger than in urea **2** thus precluding the formation of additional intermolecular hydrogen bonds (Figure 3b and Table S4 in the SI).

In the case of previously reported urea *ent*-**10** (Figure 2d[25]), the bulky R' substituents ($CO_2{}^tBu$) could be responsible for the formation of a helical structure with an angle described by consecutive carbonyl groups of 174º and an angle between

consecutive mean urea planes of 60^{o}, which leaves the structure with a void space inside the chain and with the *tert*-butyl ester groups pointing outwards.

On the other hand, urea **4** forms supramolecular chains where the carbonyl groups are aligned (angle of 178^{o} as shown in Figure 3c), and the urea groups are coplanar, as indicated by the value of τ, which is zero. Although it is a symmetrical urea (same substituents on both nitrogen atoms), the chain has no symmetry. This is due to the presence of additional interchain O*H*···*O*H bonds joining the supramolecular chains and leading to the formation of sheets (Figure 3c and Table S6 in the SI).

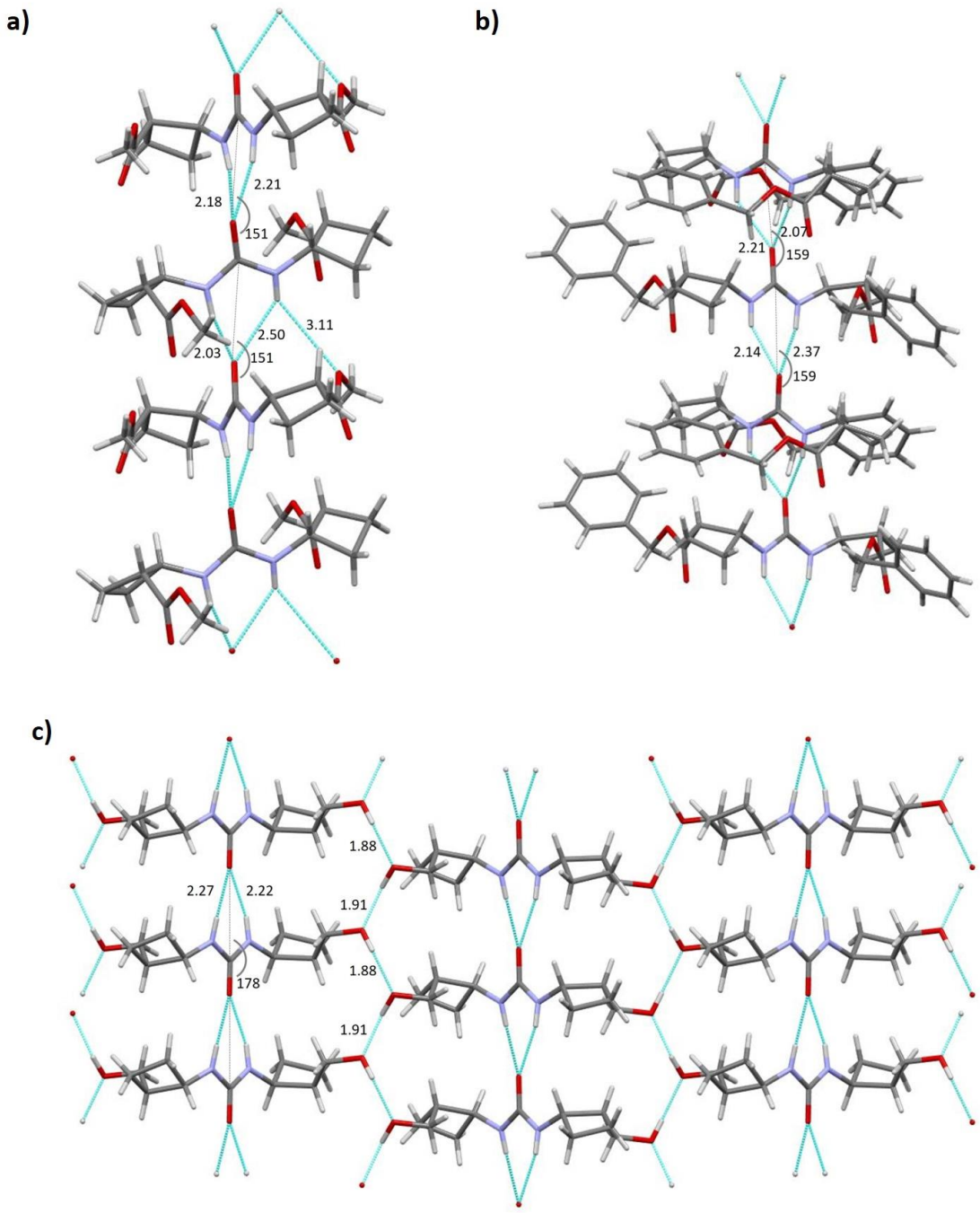

Figure 3. Supramolecular arrangements in the crystal packing of ureas: a) **2** (R' = CO_2Me); b) *ent*-**5** (R' = CO_2Bn); and c) **4** (R' = CH_2OH). R' is referred to the general formula depicted in Figure 1b. Relevant hydrogen bond distances in Å and angles in degrees.

On the contrary, in the case of urea **3**, the presence of the carboxyl groups gives rise to supramolecular chains which are significantly different from the ones discussed

above. In this case, the chains are not formed by the two N*H*···*O*C hydrogen bonds between consecutive molecules, as observed for ureas **2**, **4**, *ent*-**5** and *ent*-**10**.

The asymmetric unit of urea **3** contains 4 molecules, namely α, β, γ and δ. Two of these molecules (α and β) form chains through hydrogen bonds between one carboxyl group of one molecule and both the C*O* of the urea group and the O*H* of the carboxyl group of the consecutive molecule, defining a 12-membered ring (intrachain hydrogen bonds). In these chains, the C*O* of the carboxyl group is also intramolecularly hydrogen bonded to an N*H* of the urea group through a bifurcated bond (Figure 4a).

The chains generated by α and β molecules (α–β–α–β…) interact with another equivalent chain (α^{i}–β^{i}–α^{i}–β^{i}…) giving rise to a bigger chain. These interchain interactions involve weaker hydrogen bonds, mainly between the N*H*s of the urea groups and the carboxyl groups of the molecules of another chain as shown in Figures 4b (intrachain hydrogen bonds depicted in blue and interchain ones in green).

The other two molecules of the asymmetric unit (γ and δ) give rise to analogous chains and bigger chains with the same pattern of hydrogen bonds.

Overall, the crystal is a packing of the parallel big chains generated by α–β–α… and α^{i}–β^{i}–α^{i}… and γ–δ–γ… and γ^{i}–δ^{i}–γ^{i}, respectively, as shown in Figure 4c.

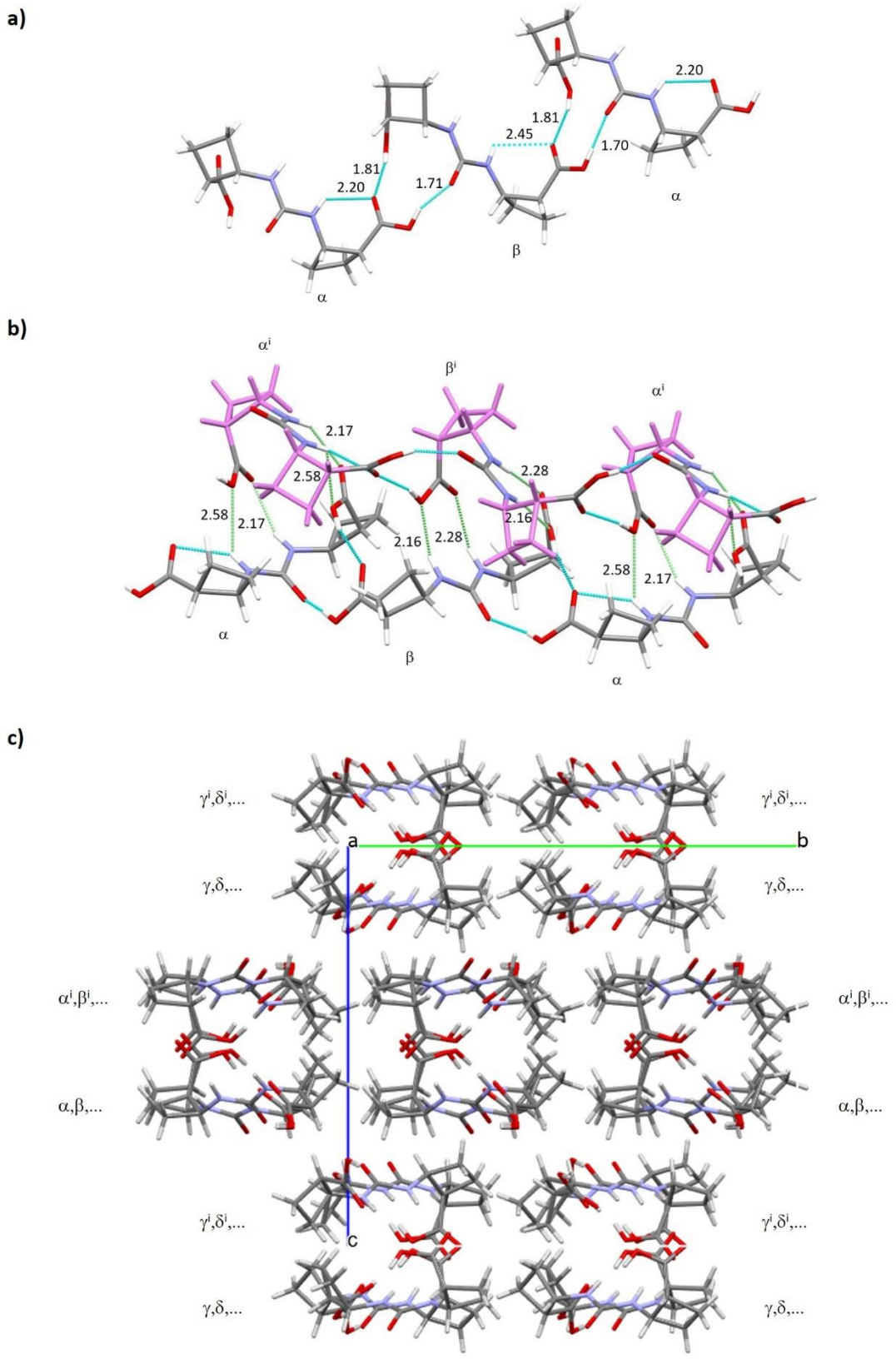

Figure 4. Supramolecular arrangements in the crystal packing of urea **3**. a) Intrachain hydrogen bonds for a chain; b) Lateral view of the interaction of two chains (one in violet and one in grey) through interchain hydrogen bonds (depicted in green); c) Packing of various chains. Relevant hydrogen bond distances in Å.

3.2.2. Computational calculations. The aim of this study was to know the energetic contribution of the main interactions leading to the crystal packing in ureas **2-5** and **10**. For simplicity, in a first step, dimeric structures were considered. On the other hand, only the enantiomers with the same chirality were investigated. Total energies of all computed structures can be found in the SI.

We started with a model urea with R' = H, for which we studied dimeric aggregates with C_2 symmetry for different torsion angles around the axis defined by the carbonyl groups (Figure 1b).

Figure 5 shows the two structures obtained. For the most stable structure **t1** the angle between mean NCON planes (τ) is 16.7º. Structure **t2** with τ = 78.5º is 2.2 kcal mol^{-1} higher in energy than **t1**. The formation energy of the **t1** structure is -12.2 kcal mol^{-1}. To assess the effect of the basis set in the geometry optimization, we have also optimized the geometries using the 6-311++G(d,p) basis set and the formation energy computed at the M06-2X/Def2TZVP level does not change.

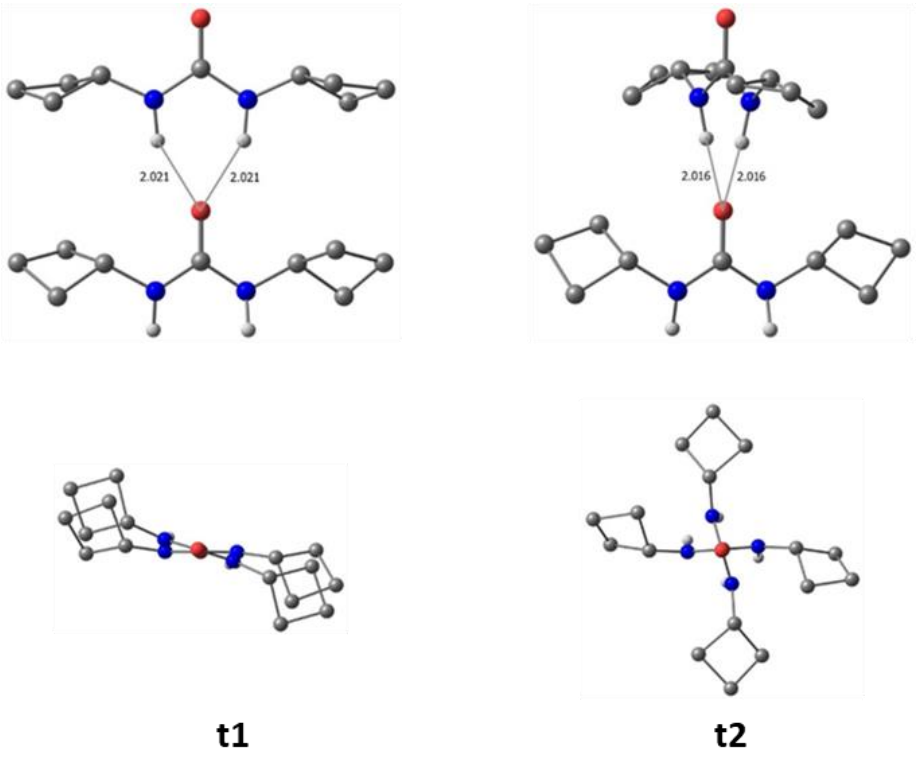

Figure 5. Side and top views of the two structures of dimeric aggregates of the model urea. Interatomic distances in Å.

Dipole-dipole interactions between both molecules should be essentially the same independently of the torsion angle. However steric repulsion between substituent groups is expected to be maximum for coplanar structures and minimum for torsion angles around 90º. Electron donor-acceptor interactions are not expected to be the most important contribution to the overall interaction (charge transfer between both urea molecules are 0.018 a.u. for **t1** and 0.014 a.u. for **t2**) but they depend on the torsion angle.

There are two main electron donor-acceptor interactions between two urea molecules (Figure 6). The first one takes place between the LP1 lone pair of oxygen and the appropriate symmetry adapted combination of antibonding orbitals $\sigma^*_{N\text{-}H}$ (*A* symmetry). The second one involves the LP2 lone pair of oxygen and the other combination of $\sigma^*_{N\text{-}H}$ orbitals (*B* symmetry). The first interaction is active independently of the torsion angle, whereas the second one reaches its maximum in a coplanar

arrangement and decreases as the torsion angle deviates from coplanarity. For τ values close to 90º the interaction involving LP2 vanishes, and the *B* symmetry adapted combination of antibonding σ^*_{N-H} orbitals may interact with the π_{CO} orbital.

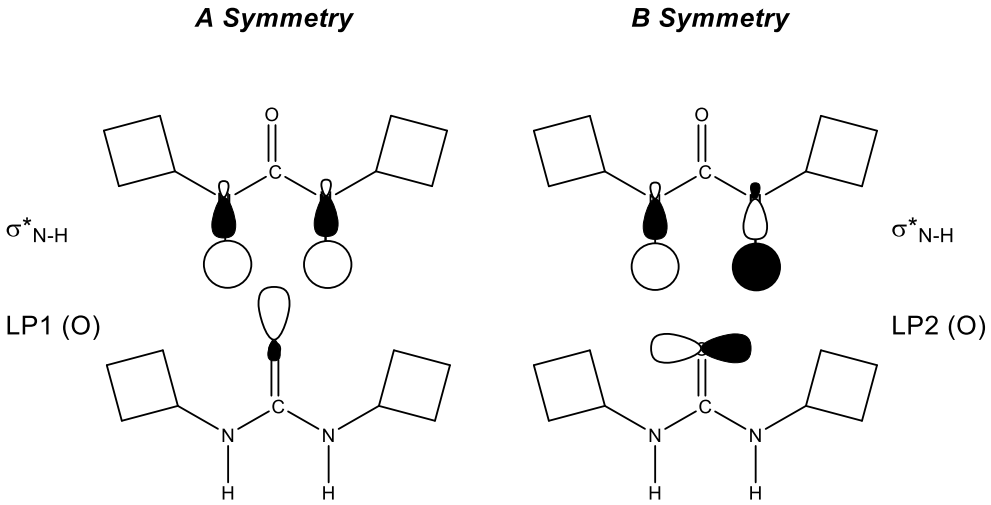

Figure 6. Electron donor-acceptor interactions between two coplanar urea molecules.

Table 1 shows the donor-acceptor interactions obtained from the second order perturbation study in the NBO basis for the two structures of dimeric aggregates of the model urea. As seen in the table, the interaction involving the π_{CO} orbital is less efficient than the one due to the LP2 (O).

Table 1. Donor-acceptor interactions (energies in kcal mol^{-1}) between two model urea molecules for structures **t1** and **t2**.

	Symmetry	**t1**	**t2**
LP1 (O) → σ^*_{N-H}	*A*	3.8	3.7
LP2 (O) → σ^*_{N-H}	*B*	2.0	
$\pi_{CO} \rightarrow \sigma^*_{N-H}$	*B*		1.1

Once the model urea was studied, we considered the three ureas where R' is an ester group: **2**, **5** and **10**. For the dimeric aggregates of these ureas we have studied two different structures: **t1** and **t2**. The results are summarized in Table 2, showing that the most stable structures are **t1** for **2** and **t2** for **5** and **10**.

The formation energy of a dimeric aggregate from two urea molecules can be decomposed into two contributions: the energy necessary to distort the fragments from their equilibrium geometry to the geometry they have in the aggregate (ΔE_{dist}) and the interaction energy between both fragments (ΔE_{int}).

For urea **2**, both the distortion and the interaction energies make **t1** the most favorable structure. On the other hand, for **5** and **10** the distortion energy favors **t2**, whereas the interaction energy favors **t1**.

Table 2. Angle between mean NCON planes (τ in degrees), formation energy (ΔE in kcal mol^{-1}) and contributions to the formation energy for dimeric aggregates of ureas **2**, **5** and **10** with C_2 symmetry.

Urea	R'	Structure	τ	ΔE_{dist}	ΔE_{int}	ΔE
2	CO_2Me	**t1**	33.0	4.7	−24.3	−19.6
		t2	77.6	7.2	−22.6	−15.5
5	CO_2Bn	**t1**	20.5	13.8	−29.6	−15.8
		t2	86.7	9.3	−25.3	−16.0
10	$CO_2{}^tBu$	**t1**	24.4	7.4	−22.5	−15.1
		t2	64.2	4.0	−21.8	−17.8

Starting from these structures, tetrameric and octameric aggregates were built and their geometries optimized. The results are summarized in Table 3.

Table 3. Average angle between mean NCON planes ($\langle\tau\rangle$ in degrees) and formation energies (in kcal mol^{-1}) for tetrameric and octameric aggregates of ureas **2**, **5** and **10** with C_2 symmetry.

Urea	R'	Structure	Tetramers		Octamers	
			$\langle\tau\rangle$	ΔE	$\langle\tau\rangle$	ΔE
2	CO_2Me	**t1**	32.7	−56.8	39.3	−131.4
		t2	80.4	−48.8	81.5	−117.1
5	CO_2Bn	**t1**	26.3	−77.2	27.5	−182.4
		t2	76.6	−78.9	82.5	−159.9
10	$CO_2{}^tBu$	**t1**	35.9	−63.6	41.1	−144.8
		t2	78.2	−59.8	63.7	−155.4

For **2**, the most stable tetrameric and octameric aggregates are **t1**, with average torsion angles between 30 and 40°, in disagreement with the crystal structure (τ = 82°).

For **5**, the most stable tetrameric aggregate is **t2**, but the situation changes for the octamer. Finally, for **10** there is also an inversion of stability between **t1** and **t2** when going from tetramer to octamer. However, the most stable octamer in in good agreement with the X-ray structure of *ent*-**10**, with $<\tau> = 63.7°$ (experimental value is 60º).

Up to this point, C_2 structures where the carbonyl groups are colinear and the N*H*···*O*C distances symmetric had been considered. However, crystal structures present significant deviation from this situation. Moreover, in the crystal structures of **2** and **5**, the angle between alternate (*i* and *i*+2 molecules in a chain) mean NCON planes is 0°, whereas for **t2** structures these angles are between 13 and 15º. We optimized the geometries of octamers in which the angle between alternate NCON planes is set to zero. These calculations lead to a remarkable deviation from the linearity of the carbonyl groups and significant asymmetry in the N*H*···*O*C hydrogen bonds along with a stabilization with respect to **t2** structures. When geometry restrictions are removed, a further stabilization is produced giving aggregates which have been named as **t2'**. The results are presented in Table 4 and the most significant geometry modifications are shown in Figure 7.

Table 4. Average angle between mean NCON planes (<τ> in degrees) and formation energies (in kcal mol^{-1}) for alternate (**t2'**) octameric aggregates of ureas **2**, **5** and **10**.

Urea	R'	<τ>	ΔE
2	CO_2Me	75.2	−131.8
5	CO_2Bn	81.8	−190.6
10	$CO_2{}^tBu$	69.8	−139.0

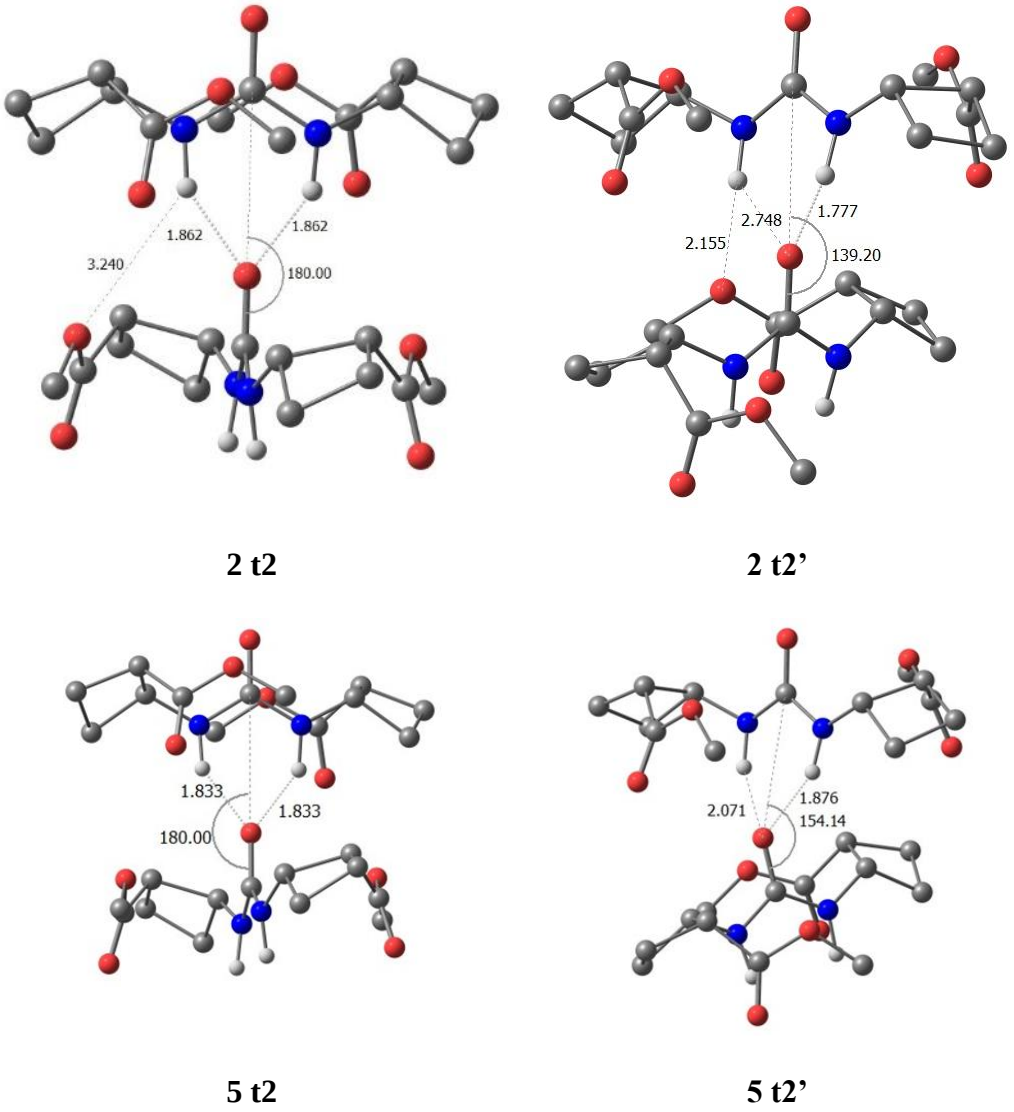

2 t2 **2 t2'**

5 t2 **5 t2'**

Figure 7. Structure of central dimer in octameric aggregate of ureas **2** and **5**. Selected distances in Å and angles in degrees. Hydrogen atoms bonded to C and phenyl group have been omitted for clarity.

In the case of urea **5**, the resultant structure is clearly more stable than the ones obtained with C_2 symmetry, whereas for **2** this non symmetric structure is only 0.4 kcal/mol more stable than **t1**. These results show that the preference for a particular aggregation pattern in urea **2** is smaller than for urea **5**.

For urea **2**, the asymmetry in the N*H*···*O*C hydrogen bond distances is maintained comparing the crystal structure and the calculated **t2'** structure (Figures 7 and 3a). Nevertheless, the difference between the two distances in the crystal structure is smaller

than in the computed one (2.0 and 2.5 Å compared to 1.8 and 2.7 Å). The degree of collinearity of the carbonyl groups is slightly smaller for the computed structure than for the crystal structure (139 º vs 151º). In the case of urea **5** (Figures 7 and 3b), one of the calculated N*H*···*O*C hydrogen bond distances for the **t2'** structure is the same as the experimental one, and the other distance is slightly shorter (2.1 and 1.9 Å compared to 2.1 and 2.4 Å). Moreover, the degree of collinearity of the consecutive carbonyl groups is very similar (154º vs 159 º).

In the crystal structure of *ent*-**10** the deviation from linearity and asymmetry of the N*H*···*O*C bonds is lower than for **2** and **5**. Moreover, this system presents a helical structure similar to **t2**. However, for **10** we also optimized structures with zero torsion angles between alternate urea molecules. In contrast to **2** and **5**, for **10** this alternate structure is clearly less stable than **t2** (see Tables 3 and 4).

Figure 8 shows the side views of the geometries of the most stable octameric aggregate of each urea (for top views of the same aggregates see Figure S5 in the SI).

To analyze the effect of the loss of C_2 symmetry in the stability of the aggregates, we have calculated the formation energies and the contributions (ΔE_{dist} and ΔE_{int}) of central dimers in octameric aggregates of ureas **2**, **5** and **10**. The results are presented in Table 5.

Table 5. Formation energy (ΔE in kcal mol^{-1}) and contributions to the formation energy for central dimers in octameric aggregates of ureas **2**, **5** and **10**.

Urea	R'		ΔE_{dist}	ΔE_{int}	ΔE
2	CO_2Me	**t1**	9.6	-22.1	-12.5
		t2	8.1	-18.9	-10.8
		t2'	12.1	-24.8	-12.6
5	CO_2Bn	**t1**	25.2	-29.9	-4.7
		t2	21.8	-22.3	-0.5
		t2'	18.5	-28.1	-9.6
10	$CO_2{}^tBu$	**t1**	10.4	-22.7	-12.4
		t2	10.7	-24.5	-13.8
		t2'	11.1	-19.4	-8.3

For **2**, the loss of symmetry involves an increase of distortion energy with respect to **t2**, but this is overcompensated by the stabilization due to the interaction energy. For **5**, in addition to the interaction energy, the distortion energy also favors the loss of symmetry. Finally, for **10** the **t2'** structure is not favorable due to the interaction energy.

Alternate **t2'** structures seem to provide a relief of steric repulsion between the ester groups of two adjacent urea molecules for **2** and **5**. This is not the case for **10**, where **t2** is the most stable structure. For the **t2** structure of **5**, the shortest and average C*H*···*H*C distances between the substituents of neighbor ureas are 2.16 and 2.29 Å, respectively. The shortest distance is below twice the van der Waals radius of H (1.10 Å).[39] For **t2'** the shortest and the average C*H*···*H*C distances are 2.23 and 2.40 Å, respectively, in such a way that steric repulsion decreases. On the other hand, for **10** the values are 2.17 and 2.32 (**t2**) and 2.17 and 2.28 (**t2'**) Å, so that no relief of steric repulsion is produced.

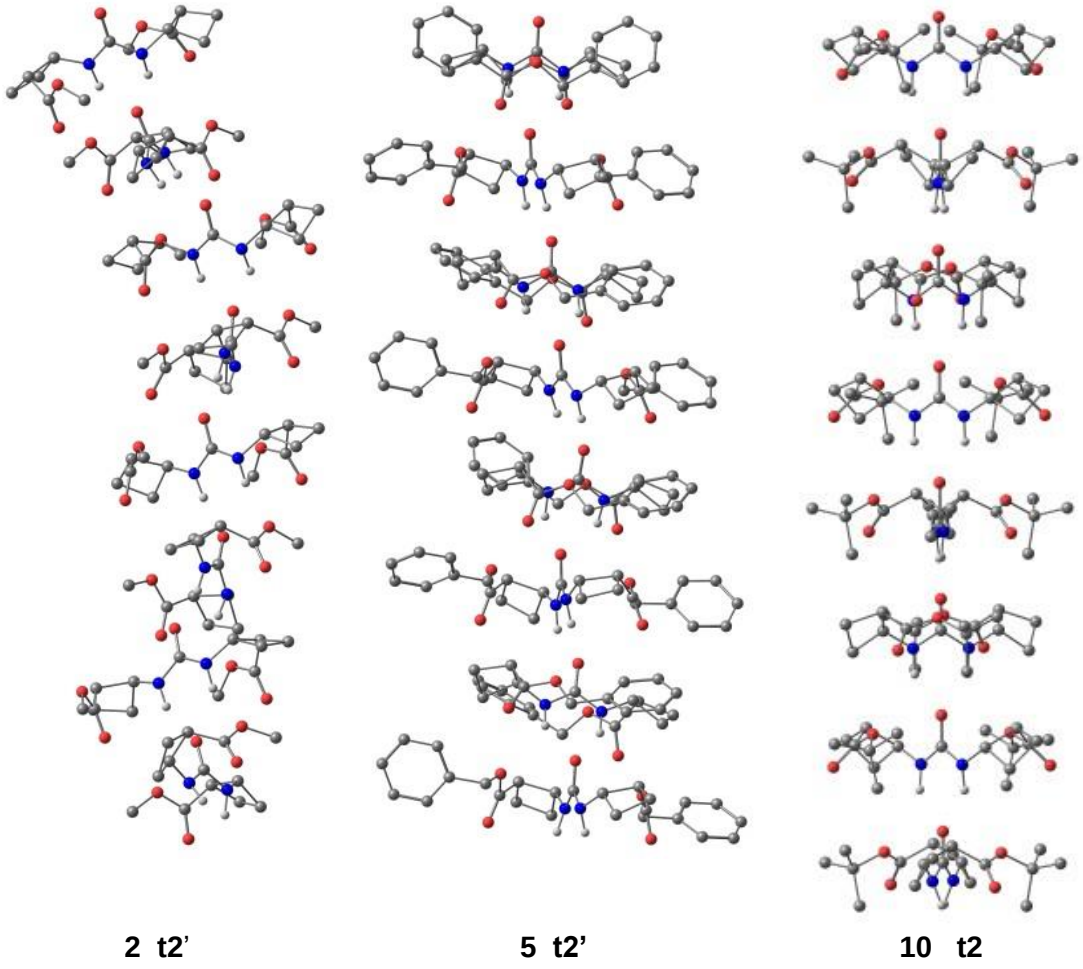

Figure 8. Side views of the most stable octameric aggregates of ureas **2**, **5** and **10**.

The two remaining ureas, **4** and **3**, where the substituents R' on the cyclobutane ring may interact through hydrogen bonding, were then considered. In both cases, dimeric aggregates with C_2 symmetry were first considered.

For urea **4**, the most stable structure corresponds to type **t2** with $\tau = 89.6^{o}$ (Figure 9). There are strong intermolecular hydrogen bond interactions between the OH groups of the side chains. This is very different from the planar structure observed in the crystal. A planar structure could be obtained by imposing geometry restrictions, and it is 2.9 kcal mol^{-1} higher in energy. When the restrictions are removed, the system evolves towards a nonsymmetric **t1'** structure ($\tau = 42.2^{o}$) which is still 2.2 kcal mol^{-1} higher in energy than **t2**.

The coplanar structure observed in the crystal structure must be due to the interactions with lateral urea molecules, which lead to the formation of a 2D hydrogen bond network. To mimic such an arrangement, the geometry of a tetrameric aggregate with two central plus two lateral urea molecules was optimized (see Figure 9). For this structure, $\tau = 17.4^{o}$. This value is not too far from the experimental $\tau = 0^{o}$ in the crystal structure. It is to be expected that increasing the size of the system in the two dimensions leads to smaller torsion angles.

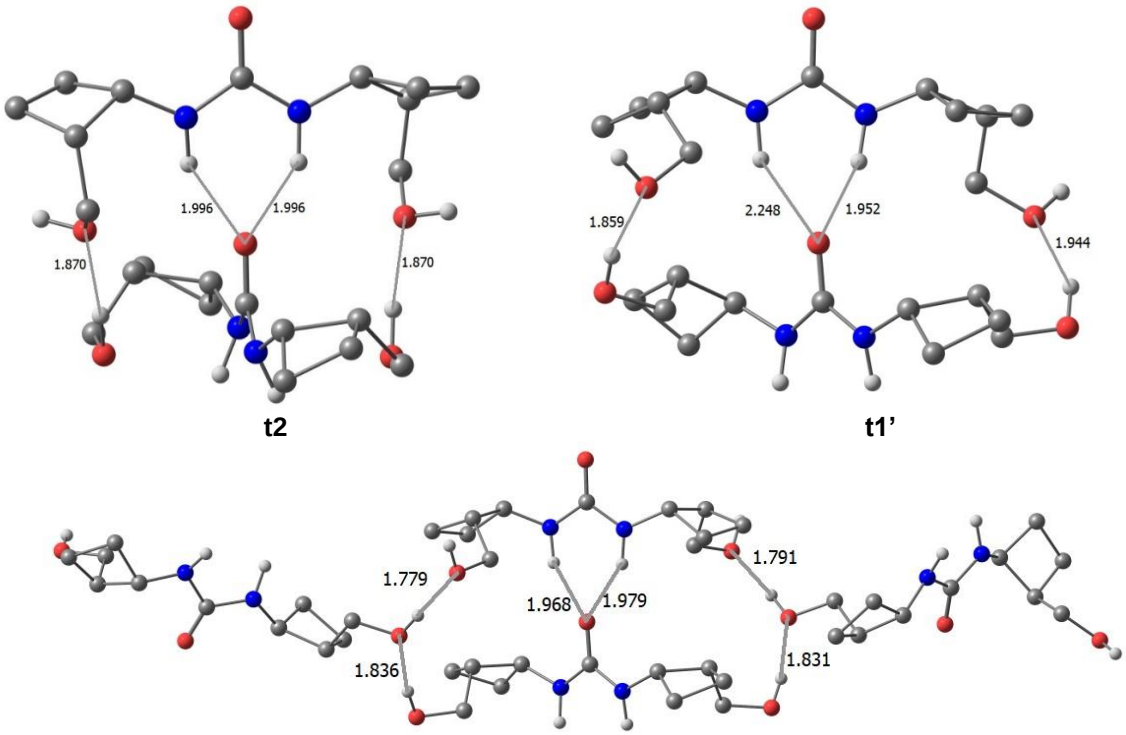

Figure 9. Structures of two dimeric and one tetrameric aggregate of urea **4**. Selected interatomic distances are in Å.

Comparing the N*H*···*O*C hydrogen bond distances in the tetrameric aggregate of urea **4** and in the X-ray structure (Figures 9 and 3c), the computed ones are slightly shorter than the experimental ones (1.9 and 1.9 Å compared to 2.3 and 2.2 Å). The hydrogen bond distances between the hydroxyl groups are very similar in both cases (1.8 Å in the

optimized tetrameric aggregate and 1.9 Å in the crystal structure). Also, the collinearity of the carbonyl groups is maintained, being in both structures close to 180º.

Regarding urea **3**, the dimeric aggregate with C_2 symmetry corresponds to a **t1** structure with a τ = 22.6º (Figure 10). In contrast with **4**, there are no hydrogen bonds involving the side groups. The most stable dimeric aggregate is the one in which the interaction between both molecules takes place through the carboxyl groups, forming the typical carboxylic acid dimers.

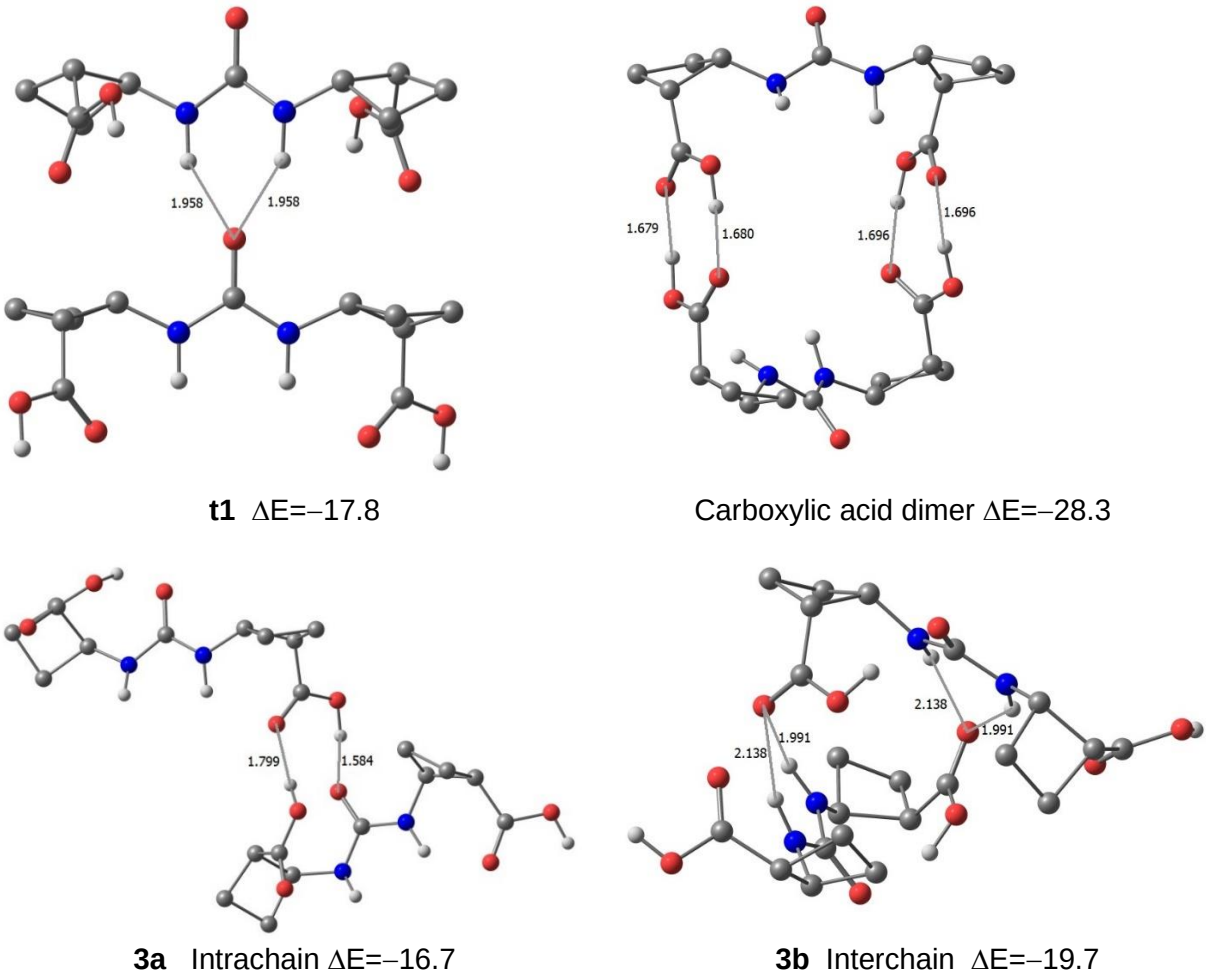

t1 ΔE=–17.8 Carboxylic acid dimer ΔE=–28.3

3a Intrachain ΔE=–16.7 **3b** Interchain ΔE=–19.7

Figure 10. Structures and formation energies (in kcal mol^{-1}) of dimeric aggregates of urea **3**. Selected interatomic distances are in Å.

The crystal structure of **3** shows that both COOH and NH groups are involved in the intermolecular interactions (Figure 4). The geometries of intrachain and interchain dimeric aggregates **3a** and **3b,** which mimic these interactions, have been optimized. The diacid dimer structure is clearly the most favored for the dimeric aggregate. However, it completely blocks the carboxylic acid groups and, therefore, its growing to yield higher aggregates does not seem to be favored. On the other hand, dimeric structures **3a** and **3b** are not so favorable, but they are able to grow to form higher aggregates. The combination of both patterns of aggregation finally leads to the observed crystal structure. The calculated hydrogen bond distances for structure **3a** are very similar to the ones observed in the crystal structure of urea **3** (1.8 and 1.6 Å compared to 1.8 and 1.7 Å; Figures 10 and 4a). Also, the hydrogen bond distances calculated for structure **3b** are very close to the experimental ones (Figures 10 and 4b).

4. CONCLUSIONS

New chiral ureas, **2**, **3**, **4** and *ent*-**5**, as well as urea **10,** have been investigated accounting for their diverse patterns of aggregation to form crystals as a function of the different abilities of the further functional groups to create intermolecular hydrogen bonding in addition to the conventional urea-urea interactions.

Compounds bearing methyl or benzyl ester groups, **2** and *ent*-**5**, respectively, form chains that are neither symmetric nor colinear or coplanar. Stabilization of these aggregates occurs mainly via the interaction energy. However, while for the methyl ester derivative **2**, both the steric repulsion between ester groups and the formation of bifurcated hydrogen bonds plays a crucial role, the higher contribution of the distortion energy favors the loss of symmetry for the benzyl derivative *ent*-**5**. Previously described compound **10**, containing *tert*-butyl esters, displays a different behavior forming helices

in which the *tert*-butyl groups are oriented towards the external wall thus minimizing the steric repulsions.

In contrast, urea **4**, with primary alcohols, makes asymmetric chains with aligned urea groups. The additional hydrogen bonding promotes the construction of sheets, and the interaction with lateral molecules leads to coplanar structures.

The most complex case corresponds to urea **3**, for which hydrogen bonding with the participation of the carboxyl groups takes place and the resulting aggregation patterns dominate. These interactions prevent the hydrogen bond arrangement observed for the other ureas studied in this work, which involves two consecutive urea groups interacting through the C*O* of one of the molecules with the two N*H* of the following one. In the case of urea **3**, molecules form chains through strong intermolecular hydrogen bonds with the participation of the carboxyl groups of one molecule and the C*O* of the urea group of the subsequent one. These chains interact amongst them through weaker hydrogen bonds involving the carboxyl groups and the N*H*s of the urea groups.

Overall, it has been shown that in most cases, 2,2'-disubstituted biscyclobutane ureas aggregate through two intermolecular N*H*···*O*C hydrogen bonds, and that the nature of the R' substituents determines the degree of deviation from the linearity of the carbonyl groups and the angle described by the NCON planes of subsequent molecules.

Thus, as a result of this study, it is concluded that the formation of twisted chains, helices or sheets in the crystals of 2,2'-disubstituted biscyclobutane ureas can be tuned by the variation of the functional groups. Alcohols form sheets, methyl and benzyl esters produce chains and bulkier tert-butyl derivatives give rise to the formation of helices. These properties are significant to be considered in the construction of materials with determined structural properties.

ASSOCIATED CONTENT

Supporting Information

^{1}H- and ^{13}C-NMR spectra of compounds **2**, **3**, **4**, *ent*-**5**, **6** and **8**; ORTEP drawings (Figures S1-S4), crystal data and structure and intermolecular hydrogen bond geometries for ureas **2**, **3**, **4** and *ent*-**5** (Tables S1-S8); Total energies (Table S9 and S10) and cartesian coordinates of computed structures; Top views of computed octameric aggregates of ureas **2**, **5** and **10** (Figure S5).

Accession Codes

CCDC 2308305 - 2308308 contain the supplementary crystallographic data for this paper. These data can be obtained free of charge via www.ccdc.cam.ac.uk/data_request/cif, or by emailing data_request@ccdc.cam.ac.uk, or by contacting The Cambridge Crystallographic Data Centre, 12 Union Road, 1038 Cambridge CB2 1EZ, UK; fax: +44 1223 336033.

AUTHOR INFORMATION

Corresponding Authors

Ona Illa – Departament de Química, Universitat Autònoma de Barcelona, 08193 Cerdanyola del Vallès, Spain; orcid.org/0000-0001-7390-4893; Email: ona.illa@uab.cat

Vicenç Branchadell - Departament de Química, Universitat Autònoma de Barcelona, 08193 Cerdanyola del Vallès, Spain; orcid.org/0000-0003-3480-1669; Email: vicenc.branchadell@uab.cat

Authors

Eric Da Silva – Departament de Química, Universitat Autònoma de Barcelona, 08193 Cerdanyola del Vallès, Spain; *Current address:* SNF, Lyon

Elisabeth Torres – Departament de Química, Universitat Autònoma de Barcelona, 08193 Cerdanyola del Vallès, Spain; *Current address: Berry Global, Inc., c/ Tuset, 23, 08006 Barcelona, Spain.*

Ángel Álvarez-Larena – Servei de Difracció de RX, Universitat Autònoma de Barcelona, 08193 Cerdanyola del Vallès, Spain; orcid.org/0000-0002-1906-0180

Klaus Wurst – Institut für Allgemeine Anorganische und Theoretische Chemie, Universität Innsbruck, A-6020, Innrain 80-82, Austria; orcid.org/0000-0002-8774-9051

Rosa M. Ortuño – Departament de Química, Universitat Autònoma de Barcelona, 08193 Cerdanyola del Vallès, Spain; orcid.org/0000-0001-7635-7354

Author Contributions

The manuscript was written through contributions of all authors. All authors have given approval to the final version of the manuscript.

Notes

The authors declare no competing financial interest.

ACKNOWLEDGMENTS

The authors would like to thank the helpful discussions with Profs. David B. Amabilino and Josep Puigmartí-Luis.

REFERENCES

(1) Mayans, E.; Gargallo, A.; Álvarez-Larena, Á.; Illa, O.; Ortuño, R. M. Diastereodivergent synthesis of chiral cyclobutane scaffolds: 1,3-amino alcohols, 1,3-diamines and some derivatives. *Eur. J. Org. Chem*. **2013**, 1425–1433. DOI: 10.1002/ejoc.201201307.

(2) Bécart, D.; Diemer, V.; Salaün, A.; Oiarbide, M.; Nelli, Y. R.; Kauffmann, B.; Fisher, L.; Palomo, C.; Guichard, G. Helical oligourea foldamers as powerful hydrogen bonding catalysts for enantioselective C-C bond-forming reactions. *J. Am. Chem. Soc*. **2017**, *139*, 12524-12532. DOI: 10.1021/jacs.7b05802.

(3) Wageling, N. B.; Decato, D. A.; Berryman, O. B. Steric effects of pH switchable, substituted (2-pyridinium)urea organocatalysts: a solution and solid-phase study. *Supramol. Chem.* **2018**, *30*, 1004-1010. DOI: 10.1080/10610278.2018.1515488.

(4) Atashkar, B.; Zolfigol, M. A.; Mallakpour, S. Applications of biological urea-based catalysts in chemical processes. *Mol. Catal*. **2018**, *542*, 192-246. DOI: 10.1016/j.mcat.2018.03.009.

(5) Kutateladze, D. A.; Strassfeld, D. A.; Jacobsen, E. N. Enantioselective tail-to-head cyclizations catalyzed by dual-hydrogen-bond donors. *J. Am. Chem. Soc.* **2020**, *142*, 6951-6956. DOI: 10.1021/jacs.0c02665.

(6) Joshi, H.; Yadav, A.; Das, A.; Singh, V. K. Organocatalytic asymmetric hetero-Diels-Alder reaction of in situ generated dienes: access to α,β-unsaturated δ-lactones featuring CF_3-substituted quaternary stereocenter. *J. Org. Chem.* **2020**, *85*, 3202-3212. DOI: 10.1021/acs.joc.9b03076.

(7) Diemer, V.; Fisher, L.; Kauffmann, B.; Guichard, G. Anion recognition by aliphatic helical oligoureas. *Chem. Eur. J.* **2016**, *22*, 15684-15692. DOI: 10.1002/chem.201602481.

(8) Ramirez Cortes, F.; Eigner, V.; Curinova, P.; Himl, M. Structurally forced ion binding affinity: tetraurea-based macrocycle as a receptor for ion pairs. *Eur. J. Org. Chem.* **2022**, *23*, e202200422. DOI: 10.1002/ejoc.202200422.

(9) Yokoya, M.; Kimura, S.; Yamanaka, M. Urea derivatives as functional molecules: supramolecular capsules, supramolecular polymers, supramolecular gels, artificial hosts, and catalysts. *Chem. Eur. J.* **2021**, *27*, 5601-5614. DOI: 10.1002/chem.202004367.

(10) Webster, C. S.; Balduzzi, F.; Davis, A. P. Tricyclic octaurea "temples" for the recognition of polar molecules in water. *Org. Biomol. Chem.* **2023**, *21*, 525-532. DOI: 10.1039/D2OB02061K.

(11) Rodriguez, J. M.; Hamilton, A. D. Benzoyl urea oligomers: synthetic foldamers that mimic extended alpha-helices. *Angew. Chem. Int. Ed*. **2007**, *46*, 8614 –8617. DOI: 10.1002/anie.200701869.

(12) Thompson, S.; Hamilton, A. D. Amphiphilic α-helix mimetics based on a benzoylurea scaffold. *Org. Biomol. Chem*. **2012**, *10*, 5780-5782. DOI: 10.1039/C2OB25273B.

(13) Fisher, L.; Guichard, G. Folding and self-assembly of aromatic and aliphatic urea oligomers: Towards connecting structure and function. *Org. Biomol. Chem***. 2010**, *8*, 3101-3117. DOI: 10.1039/C001090A.

(14) Pendem, N.; Nelli, Y.-R.; Cussol, L.; Didierjean, C.; Kauffmann, B.; Dolain, C.; Guichard, G. Synthesis and crystallographic characterization of helical hairpin oligourea foldamers. *Chem. Eur. J.* **2023**, e202300087. DOI: 10.1002/chem.202300087.

(15) Fisher, L.; Claudon, P.; Pendem, N.; Miclet, E.; Didierjean, C.; Ennifar, E.; Guichard, G. The canonical helix of urea oligomers at atomic resolution: Insights into folding-induced axial organization. *Angew. Chem. Int. Ed*. **2010**, *49*, 1067-1070. DOI: 10.1002/anie.200905592.

(16) Collie, G.; Pulka-Ziach, K.; Lombardo, C. M.; Fremaux, J.; Rosu, F.; Decossas, M.; Mauran, L.; Lambert, O.; Gabelica, V.; Mackereth, C. D.; Guichard, G. Shaping quaternary assemblies of water-soluble non-peptide helical foldamers by sequence manipulation. *Nat. Chem.* **2015**, *7*, 871-878. DOI: 10.1038/NCHEM.2353.

(17) Lombardo, C. M.; Collie, G. W.; Pulka-Ziach, K.; Rosu, F.; Gabelica, V.; Mackereth, C. D.; Guichard, G. Anatomy of an Oligourea Six-Helix Bundle. *J. Am. Chem. Soc.* **2016**, *138*, 10522-10530. DOI: 10.1021/jacs.6b05063.

(18) Yabuuchi, K.; Marfo-Owusu, E.; Kato, T. A new urea gelator: incorporation of intra- and intermolecular hydrogen bonding for stable 1D self-assembly. *Org. Biomol. Chem.* **2003**, *1*, 3464-3469. DOI: 10.1039/B307149A.

(19) Van Gorp, J. J.; Vekemans, J. A. J. M.; Meijer, E. W. C_3-symmetrical supramolecular architectures: Fibers and organic gels from discotic trisamides and trisureas. *J. Am. Chem. Soc*. **2002**, *124*, 14759-14769. DOI: 10.1021/ja020984n.

(20) See for instance: (a) Seth, S. K.; Sarkar, D.; Jana, A. D.; Kar, T. On the possibility of tuning molecular edges to direct supramolecular self-assembly in coumarin derivatives through cooperative weak forces: crystallographic and Hirshfeld surface analyses. *Cryst. Growth Des.* **2011**, *11*, 4837–4849. DOI: 10.1021/cg2006343; (b) Tripathi, S.; Islam, S.; Seth, S. K.; Bauzá, A.; Frontera, A. Mukhopadhyay, S. Supramolecular assemblies involving salt bridges: DFT and X-ray evidence of bipolarity. *CrystEngComm.* **2020**, *22*, 8171-8181. DOI: 10.1039/d0ce01356k.

(21) Groom, C. R.; Bruno, I. J.; Lightfoot, M. P.; Ward, S. C. The Cambridge Structural Database. *Acta Cryst.* **2016**, *B72*, 171-179. DOI: 10.1107/S2052520616003954.

(22) Coiro, V. M.; Giacomello, P.; Giglio, E. Determination of the molecular packing in the Crystal of *N,N'*-dicyclohexylurea by means of potential-energy calculations. *Acta Crystallogr. Cryst. Chem.* **1971**, *27*, 2112-2119. DOI: 10.1107/S0567740871005430.

(23) Goh, Y. L.; Adsool, V. A. Radical fluorination powered expedient synthesis of 3-fluorobicyclo[1.1.1]pentan-1-amine. *Org. Biomol. Chem*. **2015**, *13*, 11597. DOI: 10.1039/C5OB02066B.

(24) Huestis, M. P.; Cruz, D. D.; Di Pasquale, A. G.; Durk, M. R.; Eigenbrot, C.; Gibbons, P.; Gobbi, A.; Hunsaker, T. L.; La, H.; Leung, D. H.; Liu, W.; Malek, S.; Merchant, M.; Moffat, J. G.; Muli, C. S.; Orr, C. J.; Parr, B. T.; Shanahan, F.; Sneeringer, C. J.; Wang, W.; Yen, I.; Yin, J.; Siu, M.; Rudolph, J. Targeting KRAS mutant cancers via combination treatment: Discovery of a 5-fluoro-4-(3*H*)-quinazoline aryl urea pan-RAF kinase inhibitor. *J. Med. Chem*. **2021,** 64, 3940-3955. DOI: 10.1021/acs.jmedchem.0c02085.

(25) Izquierdo, S.; Rua, F.; Sbai, A.; Parella, T.; Álvarez-Larena, Á.; Branchadell, V.; Ortuño, R.M. (+)- and (-)-2-Aminocyclobutane-1-carboxylic acids and their incorporation into highly rigid ß-peptides: Stereoselective synthesis and a structural study. *J. Org. Chem*. **2005**, *70*, 7963-7971. DOI: 10.1021/jo0510843.

(26) Sabala, R.; Hernández, J.; Carranza, V.; Meza-Leon, R. L.; Bernes, S.; Sansinenea, E.; Ortiz, A. Rearrangement of oxazolidinethiones to thiazolidinediones or thiazinanediones and their

applications for the synthesis of chiral allylic ureas and alpha-methyl-beta-amino acids. *Tetrahedron*, **2010**, *66*, 111-120. DOI: 10.1016/j.tet.2009.11.035.

(27) See, for instance: Gorrea, E.; Pohl, G; Nolis, P.; Celis, S.; Burusco, K. K.; Branchadell, V.; Perczel, A.; Ortuño, R. M. Secondary structure of short beta-peptides as the chiral expression of monomeric building units: a rational and predictive model. *J. Org. Chem*. **2012**, *77*, 9795-9806. DOI: 10.1021/jo302034b.

(28) E. Gorrea, E.; Torres, E.; Nolis, P.; Da Silva, E.; Amabilino, D.B.; Branchadell, V.; Ortuño, R. M. Self-assembly of chiral trans-cyclobutane containing beta-dipeptides into ordered aggregates. *Chem. Eur. J*., **2011**, *17*, 4588-4597. DOI: 10.1002/chem.201002193

(29) Torres, E.; Puigmartí-Luis, J.; Pérez del Pino, Á.; Ortuño, R. M.; Amabilino, D.B. Use of unnatural beta-peptides as a self-assembling component in functional organic fibres. *Org. Biomol. Chem*. **2010**, *8*, 1661-1665. DOI: 10.1039/B922843H.

(30) Pi-Boleda, B.; Bouzas, M.; Gaztelumendi, N.; Illa, O.; Nogués, C.; Branchadell, V.; Pons, R.; Ortuño, R. M. Chiral pH-sensitive cyclobutane beta-amino acid-based cationic amphiphiles: Possible candidates for use in gene therapy. *J. Mol. Liq.* **2020**, *297*, 111856. DOI: 10.1016/j.molliq.2019.111856.

(31) Pi-Boleda, B.; Ramisetty, S. Illa, O.; Branchadell, V.; Dias, R. S.; Ortuño, R. M. Efficient DNA condensation induced by chiral β-amino acid-based cationic surfactants. *ACS Appl. Bio Mater*. **2021**, *4*, 7034-7043. DOI: 10.1021/acsabm.1c00683.

(32) Pi-Boleda, B.; Sorrenti, A.; Sans, M.; Illa, O.; Branchadell, V.; Pons, R.; Ortuño, R. M. Cyclobutane Scaffold in Bolaamphiphiles: Effect of Diastereoisomerism and Regiochemistry on Their Surface Activity and Aggregate Structure. *Langmuir*, **2018**, *34*, 11424−11432. DOI: 10.1021/acs.langmuir.8b01462.

(33) Sabbioni, G.; Jones, J. B. Enzymes in organic synthesis. 39. Preparation of chiral cyclic acid-esters and bicyclic lactones via stereoselective pig liver esterase catalyzed hydrolyses of cyclic meso diesters. *J. Org. Chem*. **1987**, 52, 4565-4570. DOI: 10.1021/jo00229a024.

(34) Experimental data coincides with that reported in: Bolm, C; Schiffers, I.; Atodiresei, I.; Hackenberg, C. P. R. An alkaloid-mediated desymmetrization of meso-anhydrides via a nucleophilic ring opening with benzyl alcohol and its application in the synthesis of highly enantiomerically enriched β-amino acids. *Tetrahedron:Asymmetry* **2003**, *14*, 3455-3467. DOI: 10.1016/S0957-4166(03)00579-2.

(35) Zhao, Y.; Truhlar, D. G. The M06 suite of density functionals for main group thermochemistry, thermochemical kinetics, noncovalent interactions, excited states, and transition elements: two new functionals and systematic testing of four M06-class functionals and 12 other functional. *Theor. Chem. Acc*. **2007**, *120*, 215–241. DOI: 10.1007/s00214-007-0310-x.

(36) Gaussian 09, Revision E.01, Frisch, M. J.; Trucks, G. W.; Schlegel, H. B.; Scuseria, G. E.; Robb, M. A.; Cheeseman, J. R.; Scalmani, G.; Barone, V.; Mennucci, B.; Petersson, G. A.*et al*. Gaussian, Inc., Wallingford CT, 2009.

(37) Weigend, F.; Ahlrichs, R. Balanced basis sets of split valence, triple zeta valence and quadruple zeta valence quality for H to Rn: Design and assessment of accuracy. *Phys. Chem. Chem. Phys.* **2005**, *7*, 3297-3305. DOI: 10.1039/B508541A .

(38) Reed, A. E.; Weinstock, R. B.; Weinhold, F. Natural population analysis. *J. Chem. Phys*. **1985**, *83*, 735-746. DOI: 10.1063/1.449486.

(39) Mantina M.; Chamberlin, A. C.; Valero; R. Cramer, C. J.; Truhlar, D. G. Consistent van der Waals radii for the whole main group. *J. Phys. Chem. A* **2009,** *113,* 5806–5812. DOI: 10.1021/jp8111556.

For Table of Contents only

Chiral Cyclobutane-Based Ureas as Versatile Platforms to Tune Structural Diversity: An Experimental and Theoretical Approach

Ona Illa, Eric Da Silva, Elisabeth Torres, Ángel Álvarez-Larena, Klaus Wurst, Rosa M. Ortuño, Vicenç Branchadell

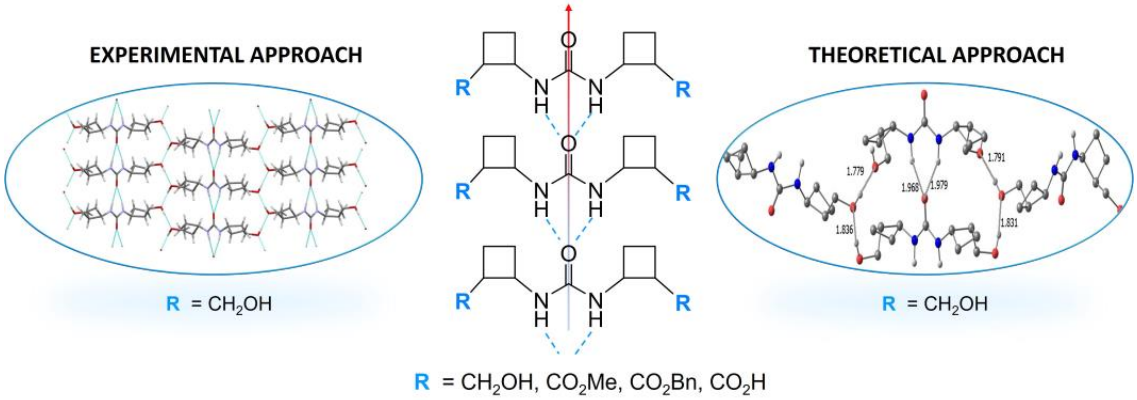

Four new chiral 2,2'-disubstituted biscyclobutane ureas have been synthesized and crystallized. The different substituents on positions 2,2' define their mode of aggregation in the crystal packing, which is governed both by the intermolecular hydrogen bonds between the urea groups and by the different ability of the substituents to generate extra hydrogen bonding. Experimental results have been rationalized with computational calculations.